Biotechnology and Bioprocess Engineering 23: 72-78 (2018)
DOI 10.1007/s12257-017-0313-y

pISSN 1226-8372
eISSN 1976-3816

RESEARCH PAPER

Removal of Feedback Inhibition of *Corynebacterium glutamicum* Phosphoenolpyruvate Carboxylase by Addition of a Short Terminal Peptide

Deyu Xu, Jing Zhao, Guoqiang Cao, Jinyu Wang, Qinggang Li, Ping Zheng, Shuxin Zhao, and Jibin Sun

Received: 7 August 2017 / Revised: 18 October 2017 / Accepted: 1 November 2017

Abstract Phosphoenolpyruvate carboxylase (PEPC) catalyzes the carboxylation of phosphoenolpyruvate (PEP) in the presence of bicarbonate to form oxaloacetate (OAA), and it plays an important role in high-efficient production of OAA-derived metabolites such as lysine, glutamate and succinate. However, PEPCs often suffered from serious feedback inhibition by various metabolic effectors like aspartate. Here, the feedback inhibition of PEPC from *Corynebacterium glutamicum* was removed by adding a short terminal peptide like His-tag. The effect of His-tag location on the structure and important properties such as activity, thermostability and feedback inhibition of PEPC has been investigated. The purified untagged PEPC, N-terminal His-tagged PEPC (PEPC-N-His) and C-terminal His-tagged PEPC (PEPC-C-His) were characterized. PEPC-N-His (439.71/sec/mM) showed a 1.26 and 186-fold higher catalytic efficiency than untagged PEPC (348.59/sec/mM) and PEPC-C-His (2.36/sec/mM), respectively. Both PEPC-N-His and untagged PEPC were significantly inhibited by aspartate at the concentrations above 4 mM (residual activities < 10%), while PEPC-C-His was almost desensitized to aspartate within 10 mM (around 90% of residual activity). Structural analysis showed that the extension of C-terminus may cause steric hindrance for aspartate binding with enzymes, leading to the deregulation of feedback inhibition of PEPC-C-His. This study provides a deeper understanding of the effect of terminal fragments on the structure and function of PEPCs, and helps to engineer the feedback inhibition of PEPCs and structurally similar enzymes.

Keywords: *Corynebacterium glutamicum*, feedback inhibition, His-tag, phosphoenolpyruvate carboxylase, structural analysis

Deyu Xu†, Shuxin Zhao
Key Laboratory of Industrial Fermentation Microbiology, Ministry of Education, College of Biotechnology, Tianjin University of Science and Technology, Tianjin 300-457, China

Deyu Xu, Jing Zhao†, Guoqiang Cao, Jinyu Wang, Qinggang Li, Ping Zheng*, Jibin Sun
Key Laboratory of Systems Microbial Biotechnology, Chinese Academy of Sciences, Tianjin 300-308, China
Tel: +86-22-8486-1994; Fax: +86-22-8486-1943
E-mail: zheng_p@tib.cas.cn

Jing Zhao, Guoqiang Cao, Jinyu Wang, Qinggang Li, Ping Zheng, Jibin Sun
Tianjin Institute of Industrial Biotechnology, Chinese Academy of Sciences, Tianjin 300-308, China

†These authors contributed equally to this work.

1. Introduction

Phosphoenolpyruvate carboxylases (PEPCs; EC 4.1.1.31) catalyze the carboxylation of phosphoenolpyruvate (PEP) to form oxaloacetate (OAA) and Pi using Mg^{2+} or Mn^{2+} as a cofactor [1]. They are present in photosynthetic organisms, nonphotosynthetic bacteria and protozoa and usually composed by four identical subunits [2]. PEPCs primarily play an anaplerotic role by replenishing C_4-dicarboxylic acids utilized for both energy and biosynthetic metabolisms and most PEPCs are allosteric enzymes with a wide variety of allosteric effectors [1,3]. Given the physiological importance of PEPCs, a large number of enzymological studies have been carried out [4,5]. The PEPC from *Corynebacterium glutamicum* (an important amino acid-producing strain) plays an important role in industrial production of OAA-derived metabolites such as lysine, glutamate and succinate [6,7]. For instance, Chen *et al*.

constructed several aspartate-resistant mutants of PEPC from *C. glutamicum* by rational protein design, and obtained a 37% higher lysine production using the strain expressing the PEPC mutant (N917G) [6].

Affinity tags particularly the short peptide like histidine-tags (His-tags) are commonly used for fast enzyme purification [8-10]. They are usually added at the N- or C-terminus of the enzyme of interest. His-tags are generally supposed to have no or little influence on the structure and function of native proteins [11]. However, His-tags can also significantly affect the solubility or catalytic activity of some specific enzymes [12-14]. Since structural analysis suggested that C-terminus of PEPCs plays an important role both in catalytic activity and allosteric regulation [15], the effect of a short terminal peptide (*e.g.,* His-tag) extension on the multiple important properties of PEPCs would be of great interest.

In this study, the purified untagged PEPC from *C. glutamicum* was compared with the N-terminal His-tagged PEPC (PEPC-N-His) and C-terminal His-tagged PEPC (PEPC-C-His) in terms of activity, feedback inhibition and thermostability. The structural basis of the His-tag effect was further elucidated.

2. Materials and Methods

2.1. Chemicals and strains

All chemicals were of analytical grade or higher quality and purchased from Sigma-Aldrich Chemie (Missouri, USA) and Solarbio (Beijing, China) unless specified. *Escherichia coli* DH5α strain was used as cloning host. For expression, *E. coli* Rosetta2 (DE3) or *E. coli* BL21 (DE3) (TransGen Biotech, Beijing, China) was used.

2.2. Construction of over-expression plasmids

The sequence of *ppc* gene from *C. glutamicum* Z188 has been deposited in NCBI database (Accession No. AKXP01000022, complement (37514-40273)) and shown in Supplementary Information. Note that the PEPC from *C. glutamicum* Z188 shares 98% amino acid sequence identity with PEPC from *C. glutamicum* ATCC13032 (Supplementary Fig. S1). The *ppc* gene from *C. glutamicum* Z188 was amplified by *ppc*-F (5'-GGAATTCCATATGACTGATTTTCTACGCGATGA CATCAGG-3') and *ppc*-R (5'-GCGTCGACCTAGCCG GAGTTGCGCAGTG-3'), the underlines indicate *Nde*I and *Sal*I restriction site, respectively. The PCR product was digested by *Nde*I and *Sal*I, and ligated into pET-28a(+) vector to obtain the recombinant plasmid for expression of PEPC with an N-terminal His-tag (named pSXG1). Additionally, the treated PCR product was ligated into pET-21a(+) vector to obtain the recombinant plasmid for expression of PEPC with a C-terminal His-tag (named pSXL2). The amino acid sequence of extended C- and N-terminus is VDKLAAALEHHHHHH and MGSSHHHHH HSSGLVPRGSH, respectively.

2.3. Expression and purification of enzymes

For protein expression, pSXG1 and pSXL2 plasmids were transformed to chemically competent *E. coli* Rosetta2 (DE3) and *E. coli* BL21 (DE3) cells, respectively. The cells were cultured in LB medium at 37°C until the optical density at 600 nm (OD_{600}) reached 0.6, and 0.5 mM IPTG (isopropyl-β-D-1-thiogalactopyranoside) was added to induce enzyme overexpression for another 24 h at 20°C. The N- or C-terminal His-tagged PEPCs were purified by using Ni-NTA resin (GE Healthcare, Uppsala, Sweden) on an AKTA purification system (GE Healthcare, Uppsala, Sweden). To obtain the purified untagged PEPC, the His-tag of PEPC-N-His was removed by thrombin digestion as shown in literature [16] with minor changes: a) the thrombin cleavage buffer was 100 mM Tris/HCl (pH 7.5) containing 20% (v/v) glycerol; b) digestion was performed at 4°C for 12 h. The enzyme purity was estimated by 12% SDS–PAGE, and enzyme concentration was measured using Pierce BCA Protein Assay Kit (Thermo Scientific, Waltham, USA).

2.4. Enzyme activity assay

The enzyme activity of the purified PEPC was determined by a coupling reaction catalyzed by malate dehydrogenase at 30°C as previously described [17,18]. PEPC catalyzes the carboxylation of PEP to form oxaloacetate and inorganic phosphate using Mn^{2+} as a cofactor, and then malate dehydrogenase catalyzes the oxaloacetate to form malate using NADH as a cofactor. The standard reaction mixture contained 100 mM Tris/HCl (pH 7.5), 2 mM PEP, 10 mM $NaHCO_3$, 10 mM $MnSO_4$, 0.1 mM NADH, 20% (v/v) glycerol, 1.6 U of malate dehydrogenase and appropriate amounts of purified PEPCs. The activity was assayed spectrophotometrically by monitoring the decrease in absorbance of NADH at 340 nm. One unit (U) of the enzyme activity was defined as the oxidization of 1 μmol of NADH per minute under assay conditions. The kinetic parameters of purified PEPCs were determined by assaying the activity on the substrate PEP at different concentrations (0.05 ~ 3 mM) but at fixed Mn^{2+} (10 mM) and $NaHCO_3$ (10 mM) concentrations. Data were fitted to the Michaelis–Menten equation by non-linear regression analysis in Graphpad Prism 6.

2.5. Thermostability

The thermostability was studied by incubating the purified enzymes in the buffer (100 mM Tris/HCl (pH 7.5), 20% (v/v) glycerol) at 30 or 40°C. Aliquots were withdrawn at

Table 1. Kinetic parameters of PEPC from *C. glutamicum* with PEP

Enzyme	Kinetic parameters[a]		
	K_m (mM)	k_{cat} (/sec)	k_{cat}/K_m (/sec/mM)
Untagged PEPC	0.41 ± 0.10	142.92 ± 8.29	348.59 ± 23.78
PEPC-N-His	0.31 ± 0.02	136.31 ± 10.32	439.71 ± 20.45
PEPC-C-His	1.95 ± 0.34	4.61 ± 1.63	2.36 ± 0.73

[a]To determine the kinetic experiments, a range of PEP concentration from 0.05 to 3 mM was assayed with a fixed concentration of $MnSO_4$ (10 mM) and $NaHCO_3$ (10 mM). All of the assays were repeated three times, and the mean values are shown.

different time intervals and the residual activities were determined as described above [19,20].

2.6. Oxaloacetate production using cell-free extracts of PEPCs

All the reactions, including 100 mM Tris/HCl buffer (pH 7.5), 6 mM PEP, 30 mM $NaHCO_3$, 30 mM $MnSO_4$, 1.2 mM NADH, 20% (v/v) glycerol, 6.4 U of malate dehydrogenase and 4.95 μg cell-free extracts of enzymes, were carried out in a total volume of 200 μL at 30°C and 800 rpm. The concentration of oxaloacetate was determined by monitoring the decrease in absorbance of NADH at 340 nm. The decrease in absorbance of NADH using supernatant of *E. coli* cells with empty vector has been determined as control, and net decrease in absorbance (after subtraction of background value) was used for oxaloacetate quantification assay.

2.7. Structural analysis

Since the structure of PEPC from *C. glutamicum* has not been elucidated until now, three-dimensional structures of untagged PEPC, PEPC-N-His and PEPC-C-His were generated by using YASARA program [21] based on the crystal structure of maize PEPC (PDB code: 1JQO) [22] or *Flaveria trinervia* PEPC (PDB code: 4BXH) [23]. PEPC from *C. glutamicum* Z188 showed 33% sequence identity with maize PEPC and 32% identity with *Flaveria trinervia* PEPC. The structures were visualized and analyzed using Pymol.

3. Results and Discussion

3.1. Catalytic activities of PEPCs

The untagged PEPC, N- and C-terminal His-tagged PEPC from *C. glutamicum* (PEPC-N-His and PEPC-C-His) were purified to electrophoretic homogeneity (Supplementary Fig. S2), and their kinetic parameters were determined. As shown in Table 1, PEPC-N-His showed a slightly higher catalytic efficiency k_{cat}/K_m (439.71 *vs*. 348.59/sec/mM) and a lower K_m (0.31 *vs*. 0.41 mM) compared with untagged PEPC. In contrast, PEPC-C-His significantly differed from them with a much lower k_{cat}/K_m (2.36/sec/mM) and higher K_m (1.95 mM). These results indicate that the catalytic activity of PEPC from *C. glutamicum* was dramatically impaired by the C-terminal His-tag.

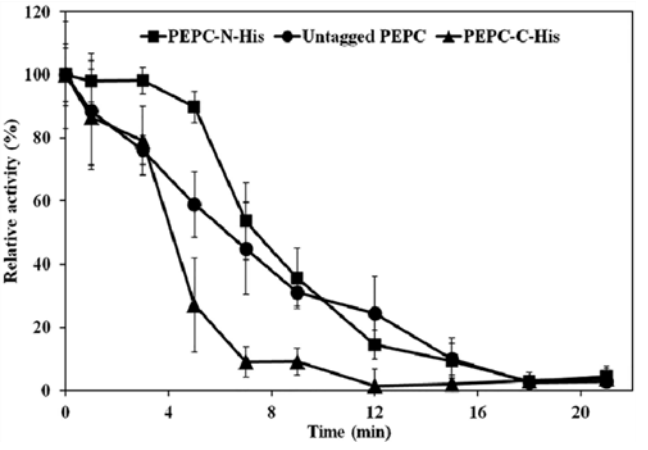

Fig. 1. Thermostability of the untagged PEPC, N- and C-terminal His-tagged PEPC at 40°C. The solutions of PEPCs were preincubated at 40°C and withdrawn at different time intervals to estimate the residual activity using the standard assay protocol. Relative activity was expressed as a percentage of the activity measured initially without any pre-incubation. All of the assays were repeated three times, and the mean values are shown.

3.2. Thermostability of PEPCs

The thermostability of PEPCs was examined by measuring the residual activities at 30 and 40°C. As shown in Supplementary Fig. S3, untagged PEPC and PEPC-N-His retained around 40% of initial activities after incubation at 30°C for 15 h, while PEPC-C-His completely lost the activity after 4 h incubation. However, all three PEPCs were heat-sensitive at 40°C, and PEPC-C-His exhibited poorer thermostability with half-life of 3 min than untagged PEPC (8 min) and PEPC-N-His (10 min) (Fig. 1). These results suggest that C-terminal His-tag may negatively affect the stability of native PEPCs. Noteworthy, many purified PEPCs were heat-sensitive at temperatures above 40°C, for example the half-lives of PEPCs from lupin were between 7 and 13 sec at 50°C [20]. In addition, the soluble PEPC-C-His was slightly less than soluble untagged PEPC (Supplementary Fig. S4), which might be caused by the poorer thermostability.

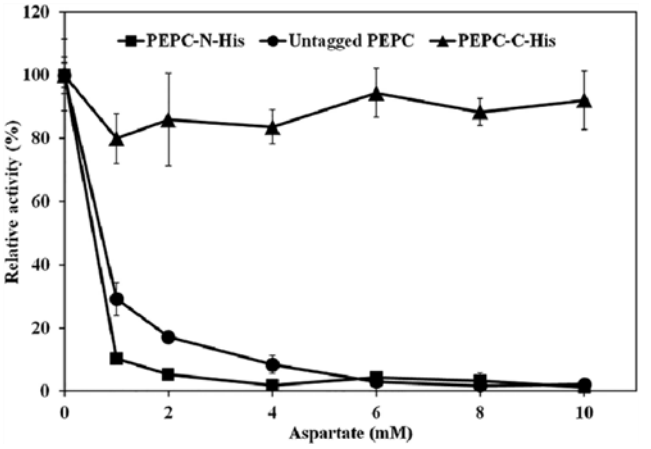

Fig. 2. Profiles of inhibition of the untagged PEPC, N- and C-terminal His-tagged PEPC by aspartate. All of the assays were repeated three times, and the mean values are shown.

3.3. Feedback inhibition of PEPCs

The residual activities of PEPCs at aspartate (an allosteric inhibitor) concentrations from 1 to 10 mM were investigated (Fig. 2). The untagged PEPC was significantly inhibited and lost most activity (> 82%) at aspartate concentrations above 2 mM, which agrees with the previous report [6]. The presence of N-terminal His-tag resulted in greater inhibition, *e.g.,* 95% of activity was lost at 2 mM aspartate. However, the inhibition was unexpectedly almost deregulated for the purified PEPC-C-His, and around 90% of activity was remained at aspartate concentrations up to 10 mM. These results suggested that the extension of a short peptide at the C-terminus of PEPCs could significantly deregulate the feedback inhibition of aspartate, but at the expense of lower catalytic efficiency in our case (C-terminal His-tag and PEPC of *C. glutamicum*). Nevertheless, the catalytic efficiency might be improved by optimizing the length and composition of C-terminus or protein engineering technique.

3.4. Oxaloacetate production using cell-free extracts of PEPCs

Supplementary Fig. S5 shows the OAA production using cell-free extracts of untagged PEPC, PEPC-C-His and PEPC-N-His. It is found that, a much higher OAA productivity was obtained using untagged PEPC and PEPC-N-His (around 500 μM for both) compared to PEPC-C-His (around 60 μM), which might be due to the significantly higher catalytic efficiency of untagged PEPC and PEPC-N-His. Interestingly, the OAA productivity was not increased after 25 and 20 min for untagged PEPC and PEPC-N-His, respectively, while it was still increased for PEPC-C-His. These results indicate that both catalytic efficiency and aspartate resistance of PEPCs are critical for efficient production of OAA. Simultaneous improvement of the activity and feedback-resistance of PEPC by optimizing the length and composition of C-terminus and protein engineering technique is currently in progress.

3.5. Structural insights into the effect of his-tag

To investigate the structural effect of His-tag, the three-dimensional structures of untagged PEPC, PEPC-N-His and PEPC-C-His were generated by homology modeling. The crystal structure of PEPC from Maize which was thought to be in the active state (R state) [22] was selected as the template. It is observed that similar with other PEPCs [22], the N-terminus of *C. glutamicum* PEPC is distant from the active site, and C-terminus is in the enzyme interior (Supplementary Fig. S6).

As shown in Fig. 3, the active site pocket was intact in both structures of untagged PEPC and PEPC-N-His, and the PEP analog DCDP (3,3-dichloro-2- dihydroxyphosphinoylmethyl-2-propenoate) can be well accommodated. However, the extension of 15 residues at C-terminus in PEPC-C-His (V920 to H934) blocked its active site pocket (Figs. 3C and 3F), causing the reduced access probability of substrate into the active site. This was supported by the much higher K_m and lower k_{cat} of PEPC-C-His (1.95 mM and 4.61/sec) than that of PEPC-N-His (0.31 mM and 136.31/sec) and untagged PEPC (0.41 mM and 142.92/sec). Note that since the extension at C-terminus would affect the rate of substrate access to the active site and/or product release, resulting in the significantly lower k_{cat} of PEPC-C-His (almost 30-fold decreased) compared to untagged PEPC, therefore k_{cat} seems to be the predominant determinant. These results can explain the lowest catalytic activity of PEPC-C-His among three forms. Note that the importance of the C-terminal peptide of PEPCs in catalytic activity has been previously reported [24]. In addition, the presence of His-tag might disturb the natural refolding of PEPC, leading to altered thermostability.

An interesting question is why PEPC-C-His but not PEPC-N-His was desensitized to the allosteric inhibitor aspartate? The C-terminus of PEPC has been demonstrated to directly interact with the allosteric inhibitor, *e.g.,* N881 formed two H-bonds with aspartate in crystal structure of *E. coli* PEPC (PDB code: 1JQN), and G919 formed one H-bond with ethylene glycol (EDO) in structure of *F. trinervia* PEPC (PDB code: 4BXH). Thus, the extension of C-terminus in PEPC-C-His may destroy these contacts or even sterically hinder access of allosteric inhibitors. This hypothesis was supported by the observations that, when structures of untagged PEPC, PEPC-N-His and PEPC-C-His were generated based on *F. trinervia* PEPC (Fig. 4 and Supplementary Fig. S7), each of the four monomers in untagged PEPC and PEPC-N-His had an EDO molecule in

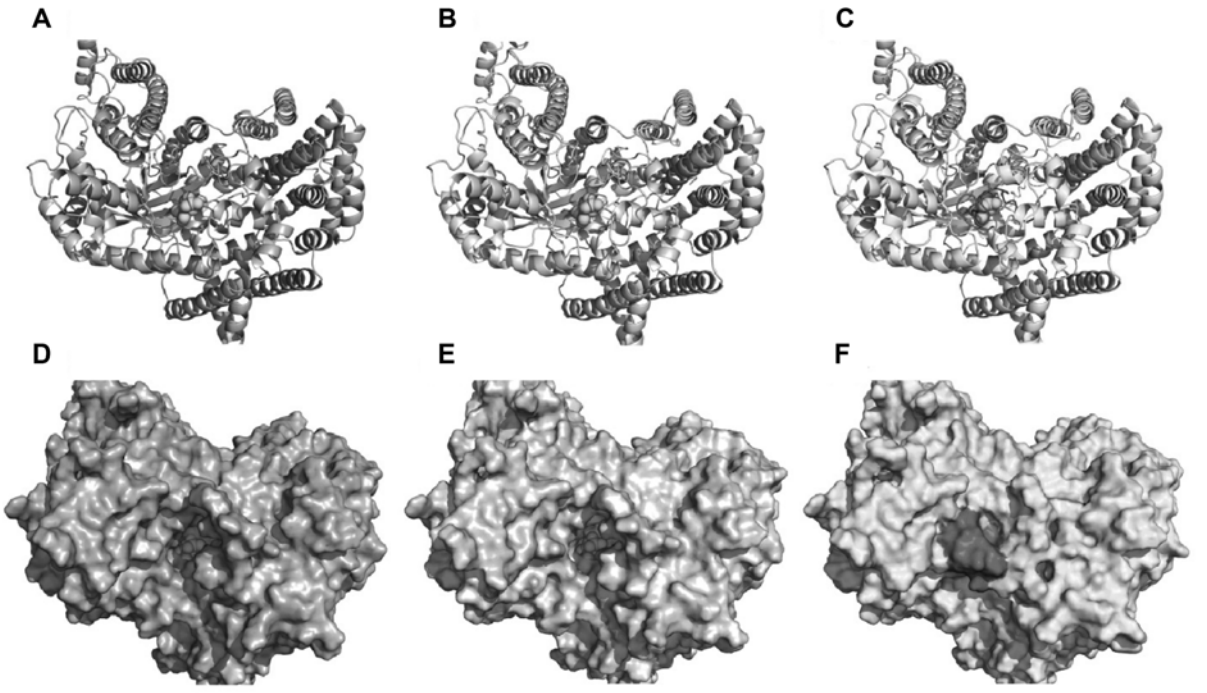

Fig. 3. Active site pocket of PEPC-N-His ((A) and (D)), untagged PEPC ((B) and (E)), and PEPC-C-His ((C) and (F)) whose structures were generated based on Maize PEPC (PDB code: 1JQO). The extension of C-terminus (V920 to H934) is in red. The PEP analog DCDP was in green sphere, and placed in active site based on its coordinates in PEPC from *E. coli* (PDB code: 1JQN). All enzyme orientations are identical and active site pocket is at the center of each structure.

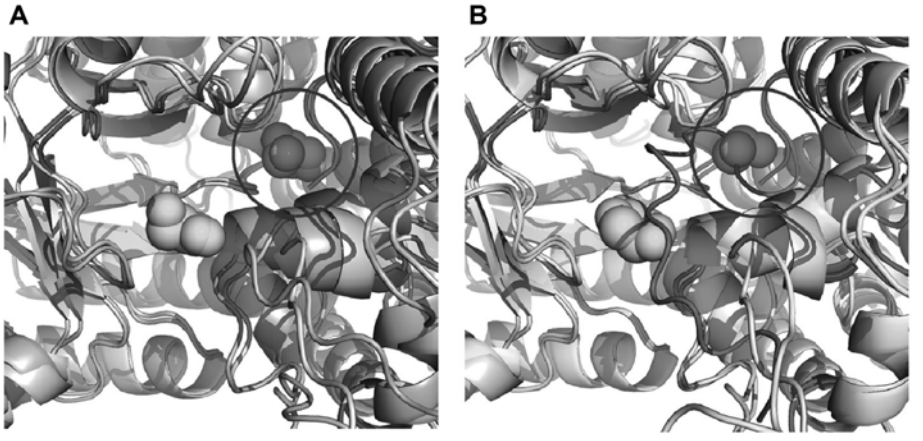

Fig. 4. Structural comparison of untagged PEPC and PEPC-N-His (A), untagged PEPC and PEPC-C-His (B) which were generated based on *F. trinervia* PEPC (PDB code: 4BXH). The untagged PEPC, PEPC-N-His and PEPC-C-His is in bluewhite, pink and cyan, respectively. The EDO in active site is in green sphere for all three structures, and EDO in inhibitor-binding site is indicated by blue circle and as the respective backbone. The extension of C-terminus (V920 to H934; VDKLAAALEHHHHHH) is in red.

inhibitor-binding site like *F. trinervia* PEPC, however such EDO molecules were absent in three of four monomers in the case of PEPC-C-His. Furthermore, another reason for the deregulation of aspartate inhibition in PEPC-C-His might be the prevention of aspartate into active site by the extended C-terminus (V920 to H934), since aspartate can function as competitive inhibitor of PEPCs [20].

Noteworthy, modification of the terminal fragments of protein has been previously reported as an alternative strategy to engineer enzyme properties of interests [25,26]. For instance, Jossek *et al.* reported a tyrosine-resistant AroF (3-deoxy-d-arabino-heptulosonate -7-phosphate synthase isoenzyme) mutant, which was obtained by removing seven N-terminal residues [25]. In another study, Zhang *et al*. constructed nine AroF mutants with truncation of different N-terminal fragments, and overexpression of the

mutant AroF$^{\Delta(1-11)}$ significantly increased the accumulation of l-phenylalanine [26]. These examples suggest that extension or deletion of terminal peptide could be an efficient approach to engineer the properties like feedback inhibition of some enzymes.

4. Conclusion

The effect of a short peptide like His-tag on the structure and catalytic properties of PEPC from *C. glutamicum* was investigated in terms of activity, feedback inhibition and thermostability. The PEPC-N-His behaved similar with untagged PEPC, while PEPC-C-His showed lower catalytic efficiency, lower thermostability, and improved aspartate resistance compared with other two forms. Structural analysis showed that the extension of C-terminus in PEPC-C-His not only prevented substrates into the active site, but also limited the small molecules like EDO or aspartate into the inhibitor-binding site. This study provides an alternative strategy to deregulate the feedback inhibition of PEPCs and other structurally similar enzymes by modifying the terminal peptides. Removal of feedback inhibition of PEPCs can contribute to the improved production of OAA-derived chemicals such as lysine, glutamate and succinate.

Acknowledgements

We are grateful for financial support from National Natural Science Foundation of China (Nos. 21606251 and 31370113), the First Special Support Plan for Talents Development in Tianjin, High-level Innovation and Entrepreneurship Team, and Natural Science Foundation of Tianjin (No. 14JCQNJC10000). We thank Jie Zhang and Jiao Liu (Tianjin Institute of Industrial Biotechnology) for their help with enzyme purification and activity assay, respectively. We thank Dr. Jianhua Yang (Tianjin Institute of Industrial Biotechnology) for critical reading of the manuscript and fruitful discussions.

Electronic Supplementary Material (ESM) The online version of this article (doi: 10.1007/s12257-017-0313-y) contains supplementary material, which is available to authorized users.

References

1. Kai, Y., H. Matsumura, and K. Izui (2003) Phosphoenolpyruvate carboxylase: Three-dimensional structure and molecular mechanisms. *Arch. Biochem. Biophys*. 414: 170-179.
2. Bandyopadhyay, A., K. Datta, J. Zhang, W. Yang, S. Raychaudhuri, M. Miyao, and S. K. Datta (2007) Enhanced photosynthesis rate in genetically engineered indica, rice expressing pepc gene cloned from maize. *Plant Sci.* 172: 1204-1209.
3. Shirai, T., K. Fujimura, C. Furusawa, K. Nagahisa, S. Shioya, and H. Shimizu (2007) Study on roles of anaplerotic pathways in glutamate overproduction of *Corynebacterium glutamicum* by metabolic flux analysis. *Microb. Cell Fact.* 6: 1-11.
4. Dong, L. Y., T. Masuda, T. Kawamura, S. Hata, and K. Izui (1998) Cloning, expression, and characterization of a root-form phosphoenolpyruvate carboxylase from Zea mays: Comparison with the C_4-form enzyme. *Plant Cell Physiol*. 39: 865-873.
5. Bläsing, O. E., K. Ernst, M. Streubel, P. Westhoff, and P. Svensson (2002) The non-photosynthetic phosphoenolpyruvate carboxylases of the C_4 dicot *Flaveria trinervia*-implications for the evolution of C_4 photosynthesis. *Planta*. 215: 448-456.
6. Chen, Z., R. R. Bommareddy, D. Frank, S. Rappert, and A. P. Zeng (2014) Deregulation of feedback inhibition of phosphoenolpyruvate carboxylase for improved lysine production in *Corynebacterium glutamicum*. *Appl. Environ. Microbiol*. 80: 1388-1393.
7. Wada, M., K. Sawada, K. Ogura, Y. Shimono, T. Hagiwara, M. Sugimoto, A. Onuki, and A. Yokota (2016) Effects of phosphoenolpyruvate carboxylase desensitization on glutamic acid production in *Corynebacterium glutamicum* ATCC 13032. *J. Biosci. Bioeng.* 121: 172-177.
8. Cho, C. W., H. P. Sun, and D. H. Nam (2001) Production and purification of single chain human insulin precursors with various fusion peptides. *Biotechnol. Bioproc. Eng*. 6: 144-149.
9. Masuda, J., E. Takayama, A. Satoh, K. Kojima-Aikawa, K. Suzuki, and I. Matsumoto (2004) A novel expression vector, designated as pHisJM, for producing recombinant His-fusion proteins. *Biotechnol. Lett*. 26: 1543-1548.
10. Yang, J., K. Ni, D. Wei, and Y. Ren (2015) One-step purification and immobilization of his-tagged protein *via* Ni^{2+}-functionalized Fe_3O_4 @ polydopamine magnetic nanoparticles. *Biotechnol. Bioproc. Eng*. 20: 901-907.
11. Carson, M., D. H. Johnson, H. McDonald, C. Brouillette, and L. J. Delucas (2007) His-tag impact on structure. *Acta Crystallogr. D. Biol. Crystallogr*. 63: 295-301.
12. Woestenenk, E. A., M. Hammarström, S. van den Berg, T. Härd, and H. Berglund (2004) His tag effect on solubility of human proteins produced in *Escherichia coli*: A comparison between four expression vectors. *J. Struct. Funct. Genom*. 5: 217-229.
13. Freydank, A. C., W. Brandt, and B. Dräger (2008) Protein structure modeling indicates hexahistidine-tag interference with enzyme activity. *Proteins* 72: 173-183.
14. Yeon, Y. J., H. J. Park, H. Y. Park, and Y. J. Yoo (2014) Effect of His-tag location on the catalytic activity of 3-hydroxybutyrate dehydrogenase. *Biotechnol. Bioproc. Eng.* 19: 798-802.
15. Kai, Y., H. Matsumura, T. Inoue, K. Terada, Y. Nagara, T. Yoshinaga, A. Kihara, K. Tsumura, and K. Izui (1999) Three-dimensional structure of phosphoenolpyruvate carboxylase: A proposed mechanism for allosteric inhibition. *Proc. Natl. Acad. Sci*. 96: 823-828.
16. Chant, A., C. M. Kraemer-Pecore, R. Watkin, and G. G. Kneale (2005) Attachment of a histidine tag to the minimal zinc finger protein of the *Aspergillus nidulans* gene regulatory protein AreA causes a conformational change at the DNA-binding site. *Protein Expr. Purif*. 39: 152-159.
17. Lara, M. V., S. D. X. Chuong, H. Akhani, C. S. Andreo, and G. E. Edwards (2006) Species having C_4 single-cell-type photosynthesis in the chenopodiaceae family evolved a photosynthetic phosphoenolpyruvate carboxylase like that of Kranz-type C_4 species. *Plant Physiol*. 142: 673-684.
18. Endo, T., Y. Mihara, T. Furumoto, H. Matsumura, Y. Kai, and

K. Izui (2008) Maize C_4-form phosphoenolpyruvate carboxylase engineered to be functional in C_3 plants: Mutations for diminished sensitivity to feedback inhibitors and for increased substrate affinity. *J. Exp. Bot*. 59: 1811-1818.
19. Blonde, J. D. and W. C. Plaxton (2003) Structural and kinetic properties of high and low molecular mass phosphoenolpyruvate carboxylase isoforms from the endosperm of developing castor oilseeds. *J. Biol. Chem*. 278: 11867-11873.
20. Marczewski, W. (1989) Kinetic properties of phosphoenolpyruvate carboxylase from lupin nodules and roots. *Physiol. Plantarum*. 76: 539-543.
21. Krieger, E., G. Koraimann, and G. Vriend (2002) Increasing the precision of comparative models with YASARA NOVA-a self-parameterizing force field. *Proteins* 47: 393-402.
22. Matsumura, H., Y. Xie, S. Shirakata, T. Inoue, T. Yoshinaga, Y. Ueno, K. Izui, and Y. Kai (2002) Crystal structures of C_4 form maize and quaternary complex of *E. coli* phosphoenolpyruvate carboxylases. *Struct*. 10: 1721-1730.
23. Schlieper, D., K. Förster, J. K. Paulus, and G. Groth (2014) Resolving the activation site of positive regulators in plant phosphoenolpyruvate carboxylase. *Mol. Plant*. 7: 437-440.
24. Xu, W. X., S. Ahmed, H. Moriyama, and R. Chollet (2006) The importance of the strictly conserved, C-terminal glycine residue in phosphoenolpyruvate carboxylase for overall catalysis mutagenesis and truncation of GLY-961 in the sorghum C_4 leaf isoform. *J. Biol. Chem*. 281: 17238-17245.
25. Jossek, R., J. Bongaerts, and G. A. Sprenger (2001) Characterization of a new feedback-resistant 3-deoxy-D-arabino-heptulosonate-7-phosphate synthase AroF of *Escherichia coli*. *FEMS Microbiol. Lett*. 202: 145-148.
26. Zhang, C., Z. Kang, J. Zhang, G. Du, J. Chen, and X. Yu (2014) Construction and application of novel feedback-resistant 3-deoxy-D-arabino-heptulosonate-7-phosphate synthases by engineering the N-terminal domain for L-phenylalanine synthesis. *FEMS Microbiol. Lett*. 353: 11-18.